



Open Access

## ORIGINAL ARTICLE

Erectile Dysfunction

# G protein-coupled receptor kinase 2 inhibition improves erectile function through amelioration of endothelial dysfunction and oxidative stress in a rat model of type 2 diabetes

Zhi-Hua Wan\*, Yuan-Jie Zhang\*, Lin Chen, Yong-Lian Guo, Guo-Hao Li, Ding Wu, Yong Wang

Type 2 diabetes mellitus (T2DM) is a common cause of erectile dysfunction (ED). It has been demonstrated that G protein-coupled receptor kinase 2 (GRK2) overexpression contributes to diabetic endothelial dysfunction and oxidative stress, which also underlies ED in T2DM. We hypothesized that GRK2 overexpressed and attenuated endothelial function of the cavernosal tissue in a rat model of T2DM. T2DM rats were established by feeding with a high-fat diet (HFD) for 2 weeks and then administering two intraperitoneal (IP) injections of a low dose of streptozotocin (STZ), followed by continuous feeding with a HFD for 6 weeks. GRK2 was inhibited by IP injection of paroxetine, a selective GRK2 inhibitor, after STZ injection. Insulin challenge tests, intracavernous pressure (ICP), GRK2 expression, the protein kinase B (Akt)/endothelial nitric oxide synthase (eNOS) pathway, nicotinamide adenine dinucleotide phosphate (NADPH) oxidase subunit gp91<sup>phox</sup>, nitric oxide (NO), reactive oxygen species (ROS) production, and apoptosis in cavernosal tissue were examined. Less response to insulin injection was observed in T2DM rats 2 weeks after HFD. Markedly increased GRK2 expression, along with impaired Akt/eNOS pathway, reduced NO production, increased gp91<sup>phox</sup> expression and ROS generation, increased apoptosis and impaired erectile function were found in T2DM rats. Inhibition of GRK2 with paroxetine ameliorated Akt/eNOS signaling, restored NO production, downregulated NADPH oxidase, subsequently inhibited ROS generation and apoptosis, and ultimately preserved erectile function. These results indicated that GRK2 upregulation may be an important mechanism underlying T2DM ED, and GRK2 inhibition may be a potential therapeutic strategy for T2DM ED.

*Asian Journal of Andrology* (2019) 21, 74–79; doi: 10.4103/aja.aja\_69\_18; published online: 14 September 2018

**Keywords:** endothelial dysfunction; erectile dysfunction; G protein-coupled receptor kinase 2; oxidative stress; type 2 diabetes mellitus

## INTRODUCTION

Diabetes mellitus (DM) is one of the most common causes of erectile dysfunction (ED). It has been estimated that 37.5% of men with type 1 DM (T1DM) and 66.3% of men with type 2 DM (T2DM) have ED.<sup>1</sup> Moreover, DM-associated ED tends to be more severe and less responsive to phosphodiesterase type 5 (PDE5) inhibitor therapy than nondiabetic ED.<sup>2,3</sup>

The pathogenesis of ED in DM is not fully elucidated due to the multifactorial and complicated nature of DM. The mechanisms that prevail in the pathogenesis of T1DM ED and T2DM ED may differ due to the different characteristics of T1DM and T2DM, such as insulin resistance and body mass index status.<sup>4</sup> It has been demonstrated that endothelial dysfunction and increased oxidative stress play crucial roles for the development of T2DM ED.<sup>4–9</sup> Endothelial dysfunction is often characterized by a decrease in nitric oxide (NO) bioavailability resulting from decreased endothelial nitric oxide synthase (eNOS) activity or expression, or increased NO scavenging. Reactive oxygen species (ROS) reduce the availability of NO through direct or indirect

mechanisms, such as a reaction with NO to form the toxic nitrating agent peroxynitrite, promoting eNOS uncoupling, and apoptosis.<sup>10–12</sup> A recent study shows that eNOS uncoupling and increased oxidative stress via nicotinamide adenine dinucleotide phosphate (NADPH) oxidase activation occur prior to carotid artery at the early stage of T2DM in the penis, emphasizing the role of endothelial dysfunction in the pathogenesis of T2DM ED.<sup>13</sup> Therefore, new treatment strategies for T2DM ED targeting endothelial function preservation are necessary.

G protein-coupled receptor kinase 2 (GRK2), a ubiquitously expressed member of the GRKs family, has been widely investigated for its function in the phosphorylation and desensitization of G protein-coupled receptors (GPCRs) and modulation of the signal-transduction mediated by GPCRs.<sup>14</sup> Besides its typical role in GPCRs regulation, GRK2 might play important roles in endothelial cell function and insulin resistance. Liu *et al.*<sup>15</sup> reported overexpression of GRK2 reduced NO release through inhibition of the protein kinase B (Akt)/eNOS signal-transduction pathway in injured liver sinusoidal endothelial cells. Increasing evidence has demonstrated that GRK2 can modulate insulin-stimulated

transduction cascades, and its upregulation plays a relevant role in insulin resistance.<sup>16–18</sup> Inhibition of GRK2 could enhance insulin-induced phosphorylation of Akt in tissues such as muscle, liver, and adipose tissue.<sup>17,18</sup> In animal models of T2DM, Taguchi *et al.*<sup>19,20</sup> demonstrated that GRK2 is an important negative regulator of insulin-induced Akt/eNOS signaling in vascular endothelial cells, implicating its role in diabetic endothelial dysfunction. Moreover, excessive expression of GRK2 could increase NAPDH oxidase expression and subsequent cellular oxidative stress and apoptosis, all of which may further reduce the NO release and contribute to endothelial dysfunction.<sup>21,22</sup>

The selective serotonin reuptake inhibitor paroxetine has been demonstrated to efficiently inhibit GRK2 expression and activity with selectivity over other GRKs.<sup>23</sup> Here, we hypothesized that GRK2 overexpression during the development of T2DM may also contribute to the impairment of the endothelial function of the penile corpus cavernosum. We used a rat model of T2DM to investigate the upregulation of GRK2 and the effects of GRK2 inhibition by paroxetine in corpus cavernosum (CC).

## MATERIALS AND METHODS

### Animals and treatment

T2DM was induced in 6-month-old male Sprague-Dawley rats (240–260 g) by feeding with a high-fat diet (HFD; 65% of total energy from fat) for 2 weeks and then 2 intraperitoneal (IP) injections of a low dose of streptozotocin (STZ; 20 mg per kg body weight; Sigma-Aldrich, St. Louis, MO, USA) 3 days apart, followed by continuous feeding with HFD for 6 weeks, according to the method described previously.<sup>13,24</sup> The control rats ( $n = 20$ ) were fed with a standard diet (LabDietR 5001; PMI Nutrition International, St. Louis, MO, USA). T2DM rats were randomly divided into two groups ( $n = 20$  per group): (1) rats were intraperitoneally injected with paroxetine (Sigma-Aldrich) dissolved in phospho-buffered saline (PBS) at a dose of 10 mg kg<sup>-1</sup> day<sup>-1</sup> after STZ injection. This dose was selected based on the published *in vivo* study;<sup>23</sup> (2) rats were treated with saline vehicle alone. Experimental protocols complied with the National Institutes of Health Guidelines for the Care and Use of Laboratory Animals, and all procedures were approved by the Committee for Animal Care and Use in Huazhong University of Science and Technology (Wuhan, China).

Total body weight, and postprandial glucose levels from tail snip capillary blood samples were tested once every 2 weeks, and insulin resistance was tested at 2 and 8 weeks of dietary manipulation. To determine the sensitivity to a challenge of insulin, rats were intraperitoneally injected with 1 IU kg<sup>-1</sup> insulin in PBS, as described previously.<sup>25</sup> Blood glucose levels were tested at 0, 15, 30, 60, 90, and 120 min post-injection, and the percentages of the baseline glucose level before insulin administration were calculated.

### Measurement of erectile responses

Intracavernous pressure (ICP) and mean arterial blood pressure (MAP) were measured as previously described in our experiment.<sup>26</sup> Electrostimulation of the cavernous nerve (CN) was applied as voltage response to stimulation (2.5 V, 5V, and 7.5 V) at 15 Hz with a pulse width of 0.5 ms for 50 s. Three stimulations were conducted at each side of the CN. Pressure curves were collected by a data-acquisition system (Powerlab, Castle Hill, Australia). The maximal ICP/MAP, and total ICP which was determined by the area under the curve (mmHg s<sup>-1</sup>), were calculated.

After measurement, a small portion of the skin-denuded penile shaft was fixed in 10% formalin and then embedded in paraffin for histologic studies. The remaining tissue was harvested immediately for enzyme activity assay or frozen and stored at -80°C.

### Histology

Adjacent sections (5 μm) were cut in a transverse direction. For immunohistochemical examination, the sections were incubated with rabbit anti-GRK2 antibody (1:100; Sigma-Aldrich) overnight at 4°C. After being washed, the sections were incubated with the horseradish peroxidase-conjugated secondary antibody. Finally, antigen-antibody reactions were performed with 0.05% diaminobenzidine. At least three matched sections per specimen and at least three fields in each section were examined. Semi-quantitative analysis was performed using Image-Pro plus software (Media Cybernetics, Silver Spring, MD, USA).

### Real-time quantitative polymerase chain reaction

Total RNA of cavernosal tissue was isolated using TRIzol reagent (Invitrogen, Carlsbad, CA, USA). As described in our previous experiment,<sup>27</sup> the cDNA was synthesized using the PrimeScript™ RT reagent Kit (TaKaRa, Dalian, China) and real-time polymerase chain reaction (PCR) was performed using SYBR Premix Ex Taq (TaKaRa) with ABI PRISM 7900HT Sequence Detection System (Applied Biosystems, Los Angeles, CA, USA). GRK2, Akt, eNOS, gp91<sup>phox</sup>, and caspase-3 mRNA were measured. PCR was performed in at least three replicates. The 2<sup>-ΔΔCt</sup> method was used for quantification (fold difference) of the expression level.<sup>28</sup> β-actin was used as an endogenous reference gene. The PCR primers are presented in **Table 1**.

### Western blot analysis

As described previously,<sup>26,27</sup> briefly, 40 μg of total protein was transferred onto a nitrocellulose membrane (Pierce, Rocford, IL, USA) and incubated with appropriate dilutions of the primary specific antibody, including anti-Akt, anti-phospho-Akt (Thr308), anti-phospho-Akt (Ser473), anti-eNOS, anti-phospho-eNOS (Thr495), anti-phospho-eNOS (Ser1177) (1:1000, CST, Danvers, MA, USA), anti-GRK2, anti-gp91<sup>phox</sup>, anti-caspase-3, anti-active (cleaved) caspase-3 antibody (1:1000, Abcam, Cambridge, MA, USA), followed by incubation with horseradish peroxidase (HRP) conjugated secondary antibody. The membranes were then analyzed using a chemiluminescence detection system. Experiments were independently performed at least three times. The relative signal intensity was quantified by densitometry and normalized to the β-actin expression level.

### NOS activity, NO level, and caspase-3 activity assay

NOS activity, NO level, and caspase-3 activity in rat cavernosal tissue were measured using a NOS Activity Assay Kit (Fluorometric; Biovision, Milpitas, CA, USA), a Nitric Oxide Colorimetric Assay Kit (Biovision) and a Caspase-3 Assay Kit (Fluorometric; Abcam) according to the manufacturer's instructions, respectively. The assay

**Table 1: The sequences of PCR primers**

Primer	Sequence
GRK2	Forward: 5'-TGGGATCACAGGAATTGTCA-3'
	Reverse: 5'-TAGGGTACAAATGACCTCAGC-3'
Akt	Forward: 5'-TTTGGGAAGGTGATCTGGTG-3'
	Reverse: 5'-GGTCGTGGGTCTGGAATGAGT-3'
eNOS	Forward: 5'-GATCCCTAACTTGCCTTGCATCCT-3'
	Reverse: 5'-TGTAATCGGCTTGGCCAGAATCC-3'
gp91 <sup>phox</sup>	Forward: 5'-TGGGATCACAGGAATTGTCA-3'
	Reverse: 5'-CTTCCAAACTCTCCGAGTC-3'
β-actin	Forward: 5'-GGAGATTACTGCCCTGGCTCCTA-3'
	Reverse: 5'-GACTCATCGTACTCCTGCTTGCTG-3'

GRK2: G protein-coupled receptor kinase 2; Akt: protein kinase B; eNOS: endothelial nitric oxide synthase



for each specimen was performed at least three times. The results were normalized for total protein in each sample.

### ROS assay

ROS production in CC was measured as described previously.<sup>27</sup> Briefly, CC homogenate (100 µg) was added to sample wells sealed with Topseal-A (Perkin Elmer, Oak Brook, IL, USA) or background wells and then lucigenin (Sigma-Aldrich) was added at a concentration of 5 mmol l<sup>-1</sup>. Plates were counted on a scintillation counter (Perkin Elmer) set to single-photon counting mode. The assay for each specimen was performed at least three times. The results were expressed as counts per min (CPM) per mg of protein.

### TUNEL assay

Terminal deoxynucleotidyl transferase (TdT)-mediated dUTP nick end-labeling (TUNEL) assay in CC was performed using a Fluorescein DNA Fragmentation Detection Kit (Oncogene, Boston, MA, USA) according to the manufacturer's instructions. The nuclei were stained with 4,6-diamidino-2-phenylindole (DAPI). The number of apoptotic cells in the cross section were counted in five randomly selected microscopic fields at a final magnification of ×200, and the average of apoptotic cell number in five fields per sample were calculated.

### Statistical analysis

Data are analyzed by ANOVA with Student-Newman-Keuls post-hoc analysis with PASW Statistics18 software (SPSS Inc., Chicago, IL, USA) and expressed as mean ± standard deviation (s.d.). Differences were considered statistically significant when  $P < 0.05$ .

## RESULTS

### HFD plus STZ injection induced establishment of T2DM

After 4 weeks of HFD (1 week after STZ injection), markedly increased blood glucose and body weight were found in the T2DM rats ( $P < 0.05$ , **Figure 1a** and **1b**). Insulin resistance was tested at 2 and 8 weeks after HFD (**Figure 1c** and **1d**). Less response to insulin injection was observed in T2DM rats 2 weeks after HFD ( $P < 0.05$ , **Figure 1c**), although there was no marked difference in blood glucose ( $P = 0.071$ ) and body weight ( $P = 0.122$ ) at this time point, indicating the onset of insulin resistance at the early stage of T2DM.

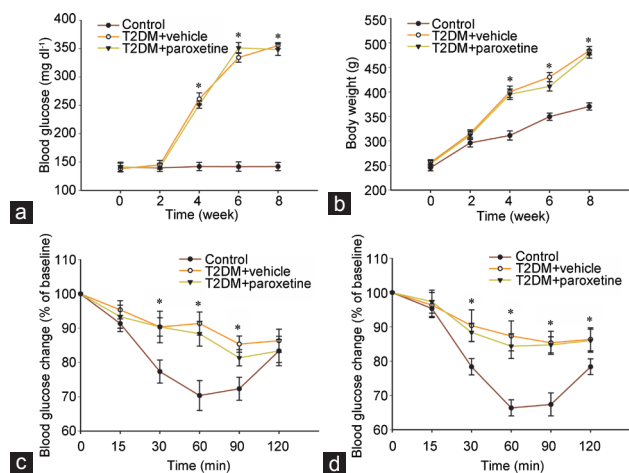


**Figure 1:** (a) Postprandial blood glucose was tested once every 2 weeks. (b) Body weight was tested once every 2 weeks. (c) An insulin challenge test was performed at 2 weeks of dietary manipulation. (d) An insulin challenge test was performed at 8 weeks of dietary manipulation. Results were reported as mean ± standard deviation (s.d.). \* $P < 0.05$ , the indicated group versus control group,  $n = 20$  per group. T2DM: type 2 diabetes mellitus.

### T2DM induced overexpression of GRK2 in the CC of T2DM rats

Localization of GRK2 in CC was determined by immunohistochemical examination (**Figure 2a**). GRK2 expression in CC was measured by real-time quantitative PCR (**Figure 2c**) and western blot analysis (**Figure 2d**). Compared with the control rats, T2DM rats showed markedly higher GRK2 immunoreactivity ( $P < 0.05$ , **Figure 2b**). Compared with the control rats, T2DM led to an approximately 3.5-fold and 2.2-fold increase in GRK2 mRNA and protein expression, respectively, whereas this increase was prevented by paroxetine treatment ( $P < 0.05$ , **Figure 2c** and **2e**).

### Chronic paroxetine treatment preserved erectile function of T2DM rats

The functional consequence of GRK2 inhibition was evaluated by CN stimulation (**Figure 3**). Both ICP/MAP and total ICP in T2DM rats were lower in contrast to nondiabetic control rats at all levels of settings (2.5 V, 5 V, and 7.5 V) ( $P < 0.05$ ). GRK2 inhibition with paroxetine had partially but markedly increased ICP/MAP and total ICP in response to CN stimulation at the 5 V and 7.5 V settings ( $P < 0.05$ ), whereas no marked difference in ICP/MAP and total ICP were found between T2DM rats and the paroxetine treatment group at low-voltage (2.5 V) stimulation ( $P = 0.232$  and  $P = 0.262$ , respectively).

### Paroxetine treatment ameliorated the Akt-eNOS pathway in CC of T2DM rats

There was no marked difference of Akt mRNA ( $P = 0.422$ ) and protein expression ( $P = 0.354$ ) and the phosphorylation of Akt at Ser473 ( $P = 0.829$ ) among the three groups, whereas the

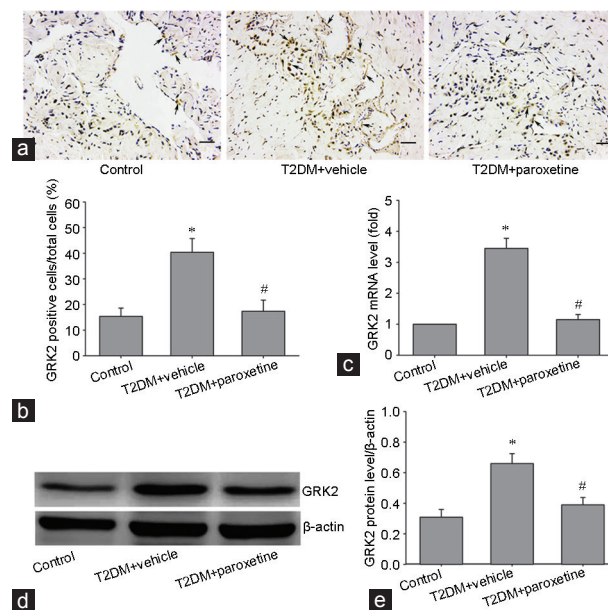


**Figure 2:** GRK2 activation in cavernosal tissue. (a) GRK2 localization was assessed by immunohistochemistry (magnification ×200, scale bars = 50 µm). (b) Bar graphs represent quantitative image analysis for immunohistochemistry. (c) The expression of GRK2 mRNA was measured by real-time quantitative PCR. The data were presented as the fold change relative to the non-diabetic control. (d) GRK2 protein expression was measured by western blot analysis. β-actin was used as a loading control. (e) Expression levels of GRK2 protein were normalized to β-actin. Results were reported as mean ± standard deviation (s.d.). \* $P < 0.05$ , the indicated group versus control group; # $P < 0.05$ , the indicated group versus T2DM+vehicle group,  $n = 20$  per group. All results are representative of three independent experiments. GRK2: G protein-coupled receptor kinase 2; T2DM: type 2 diabetes mellitus, PCR: polymerase chain reaction.

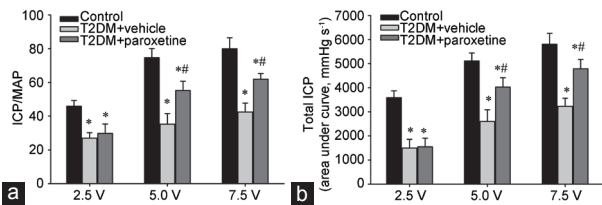


**Figure 3:** Effects of GRK2 inhibition on erectile responses to electrical stimulation. Electrostimulation of the cavernous nerve was applied as voltage response (2.5 V, 5 V, and 7.5 V) at 15 Hz with a pulse width of 0.5 ms for 50 s. Erectile response is expressed as (a) ICP/MAP and (b) total ICP. Results were reported as mean  $\pm$  standard deviation (s.d.). \* $P < 0.05$ , the indicated group versus control group; # $P < 0.05$ , the indicated group versus T2DM+vehicle group;  $n = 20$  per group. All results are representative of three independent experiments. GRK2: G protein-coupled receptor kinase 2; T2DM: type 2 diabetes mellitus; ICP: intracavernous pressure; MAP: mean arterial blood pressure.

phosphorylation of Akt at Thr308 markedly decreased in T2DM rats, and paroxetine markedly inhibited this decrease ( $P < 0.05$ , **Figure 4a–4d**). Markedly decreased eNOS mRNA and protein expression and the phosphorylation of eNOS at Ser1177, along with markedly elevated phosphorylation of eNOS at Thr495, were found in CC of T2DM rats ( $P < 0.05$ ). Paroxetine increased at least partially eNOS transcriptional level, protein expression, and the phosphorylation of eNOS at Ser1177, and partially inhibited the phosphorylation of eNOS at Thr495 ( $P < 0.05$ ). Furthermore, NOS activity and total NO production were markedly attenuated in T2DM rats, and this impairment was prevented by chronic treatment with paroxetine ( $P < 0.05$ , **Figure 4e** and **4f**).

#### Paroxetine treatment inhibited oxidative stress in CC of T2DM rats

The mRNA and protein expression level of NADPH oxidase subunit gp91<sup>phox</sup> were markedly increased in CC of T2DM rats to 4.2-fold and 5.5-fold those of the control rats, respectively ( $P < 0.05$ , **Figure 5a–5c**), and this increase was partially prevented by paroxetine treatment ( $P < 0.05$ ). Markedly elevated ROS generation was also found in CC of T2DM rats ( $P < 0.05$ , **Figure 5d**), and paroxetine treatment markedly prevented the increase ( $P < 0.05$ ), although, it remained higher than that of the control rats.

#### Paroxetine treatment reduced apoptotic cells in CC of T2DM rats

A markedly increased number of TUNEL-positive cells was found in T2DM rats ( $27 \pm 4$  per field) compared with the control rats ( $2 \pm 1$  per field) ( $P < 0.05$ ), and the number was decreased in tissues from paroxetine-treated rats ( $10 \pm 2$  per field) ( $P < 0.05$ , **Figure 6a** and **6b**). Compared with the control rats, both caspase-3 and cleaved caspase-3 protein level were markedly increased in CC of T2DM rats ( $P < 0.05$ ), and paroxetine treatment reduced the increased production partially ( $P < 0.05$ , **Figure 6c** and **6d**). Likewise, caspase-3 activity in T2DM rats was higher than that in control rats, and paroxetine could partially reduce caspase-3 activity in T2DM rats ( $P < 0.05$ , **Figure 6e**).

## DISCUSSION

In the present study, we found that there was an increased penile GRK2 expression along with impaired endothelial function and erectile function in T2DM rats. We also demonstrated that inhibition of GRK2 with paroxetine ameliorated the Akt/eNOS signaling pathway, inhibited oxidative stress and cell apoptosis in CC, thus improving endothelial function and erectile function in a rat model of T2DM, indicating that GRK2 upregulation might be an important mechanism underlying T2DM ED.

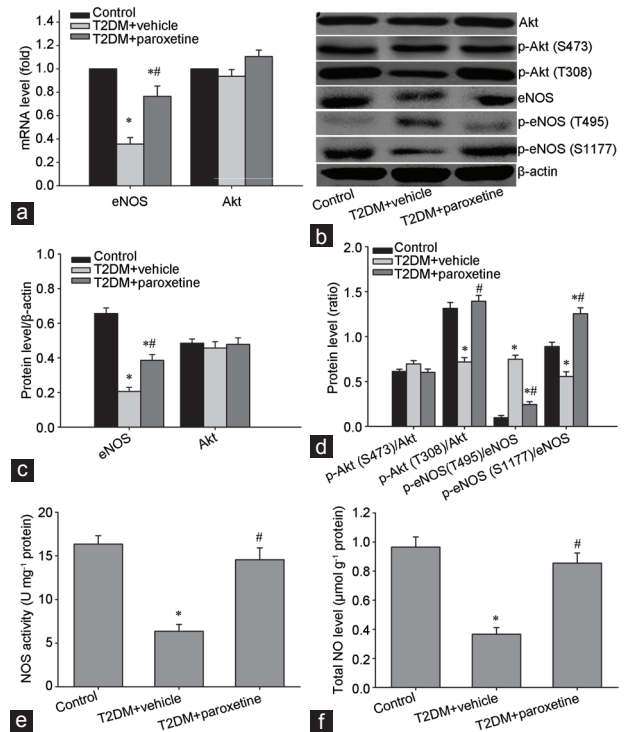


**Figure 4:** Effect of GRK2 inhibition on the Akt-NOS-NO signaling pathway. (a) The expression levels of Akt and eNOS mRNA were measured by real-time quantitative polymerase chain reaction (PCR). The data were presented as the fold change relative to the non-diabetic controls. (b) Akt, p-Akt (Thr308), p-Akt (Ser473), eNOS, p-eNOS (Thr495), and p-eNOS (Ser1177) protein expression were measured by western blot analysis.  $\beta$ -actin was used as a loading control. (c) Expression levels of eNOS and Akt protein were normalized to  $\beta$ -actin. (d) Densitometric ratios of phosphorylated Akt to total Akt and phosphorylated eNOS to total eNOS. (e) NOS activity was measured by fluorometric analysis. (f) Total NO level was measured by the colorimetric method. Results were reported as mean  $\pm$  standard deviation (s.d.). \* $P < 0.05$ , the indicated group versus control group; # $P < 0.05$ , the indicated group versus T2DM+vehicle group;  $n = 20$  per group. All results are representative of three independent experiments. GRK2: G protein-coupled receptor kinase 2; T2DM: type 2 diabetes mellitus; Akt: protein kinase B; eNOS: endothelial nitric oxide synthase; p-eNOS: phospho-eNOS; p-Akt: phospho-Akt; NO: nitric oxide.

In the context of T2DM, it has been demonstrated that endothelial dysfunction plays an important role in the development of ED. Reduced eNOS mRNA and protein expression, decreased phosphorylation of eNOS at Ser-1177 by serine-threonine protein kinase Akt, increased dissociation of functional eNOS dimers into nonfunctional monomers, and reduced NOS activity have been noticed in CC of rat or mouse models of T2DM, all of which would lead to decreased NO production.<sup>5–9,13,24</sup> Consistent with previous reports, we also found an impaired Akt-eNOS pathway in CC of T2DM rats, including reduced eNOS expression at both transcription and protein level, decreased phosphorylation of Akt at Thr308 and phosphorylation of eNOS at Ser-1177, as well as subsequent reduced total NOS activity and NO production.

In addition to the negative modulation of GPCR, GRK2 has been stressed as a nodal point of many intracellular signal transduction pathways.<sup>16,29–31</sup> In sinusoidal endothelial cells of injured liver, GRK2 overexpression inhibited Akt and eNOS phosphorylation and substantially reduced production of NO, whereas knockdown of GRK2 ameliorated Akt-eNOS-NO transduction, restored endothelial function, and normalized portal pressure; this

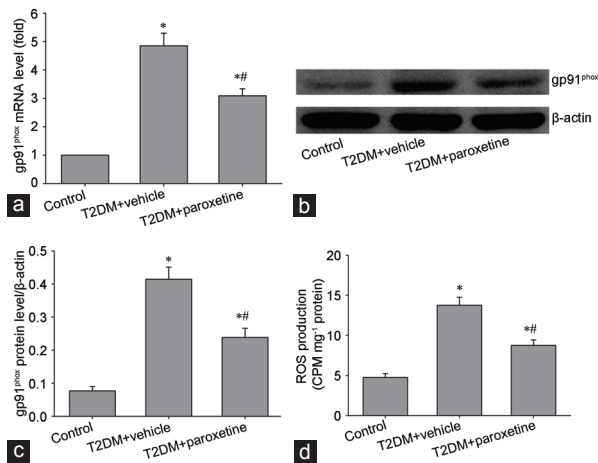


**Figure 5:** Effect of GRK2 inhibition on oxidative stress. (a) The expression of gp91<sup>phox</sup> mRNA was measured by real-time quantitative polymerase chain reaction (PCR). The data were presented as the fold change relative to the non-diabetic controls. (b) gp91<sup>phox</sup> protein expression was measured by western blot analysis. β-actin was used as a loading control. (c) Expression levels of gp91<sup>phox</sup> protein were normalized to β-actin. (d) ROS production in cavernosal tissue was expressed as CPM mg<sup>-1</sup> protein. Results were reported as mean ± standard deviation (s.d.). \**P* < 0.05, the indicated group versus control group; #*P* < 0.05, the indicated group versus T2DM+vehicle group; *n* = 20 per group. All results are representative of three independent experiments. CPM: counts per min; GRK2: G protein-coupled receptor kinase 2; T2DM: type 2 diabetes mellitus; ROS: reactive oxygen species.

suggests that overexpression of GRK2 is an important mechanism underlying endothelial dysfunction.<sup>15</sup> Under conditions of insulin resistance, elevated GRK2 expression or activity, possibly triggered by hyperinsulinemia or altered cytokine expression, impairs insulin-mediated Akt activation in endothelial cells in a kinase-activity independent way and attenuates endothelial function.<sup>16–20</sup> Consistent with studies on these pathologies, we observed a marked increase in GRK2 expression, along with an impaired Akt/eNOS pathway, in CC of T2DM and GRK2 inhibition with paroxetine-restored phosphorylation of Akt and eNOS, normalized eNOS activity, and NO production.

In addition to an impaired Akt/eNOS pathway, increased oxidative stress also underlies the endothelial dysfunction in DM.<sup>4,10–13</sup> Chronic hyperglycemia leads to excessive ROS production, in particular superoxide anion, which increases NO scavenging through reaction with NO to form the toxic nitrating agent peroxynitrite (ONOO<sup>-</sup>).<sup>27,32</sup> Peroxynitrite further causes eNOS uncoupling, resulting in the production of superoxide rather than NO.<sup>33</sup> In addition, ROS induces endothelial cell death through DNA damage, and thus amplifies the decrease in NO.<sup>4,32</sup> NADPH oxidase is a major source of ROS in the development of vascular diseases including DM and ED. Elevated expression of NADPH oxidase subunits, such as gp91<sup>phox</sup> and p47<sup>phox</sup>, has been demonstrated in the penis of T1DM or T2DM animals.<sup>8,13,27</sup>

Overexpression of GRK2 could lead to the increase in NADPH oxidase expression, ROS production, and oxidative-induced cell death in cardiac myocytes.<sup>21,22</sup> GRK2 inhibition exerts the anti-oxidative stress and anti-apoptosis effects through downregulation of NADPH oxidase and upregulation of pro-survival B cell leukemia/lymphoma 2 (Bcl-2)/Bcl-xL expression.<sup>21,22</sup> In the present study, as consistent with previous reports, we also found upregulated expression of gp91<sup>phox</sup>, along with enhanced ROS level and increased apoptosis cells, in the cavernosal tissue from T2DM rats, whereas paroxetine ameliorated these deficits markedly.

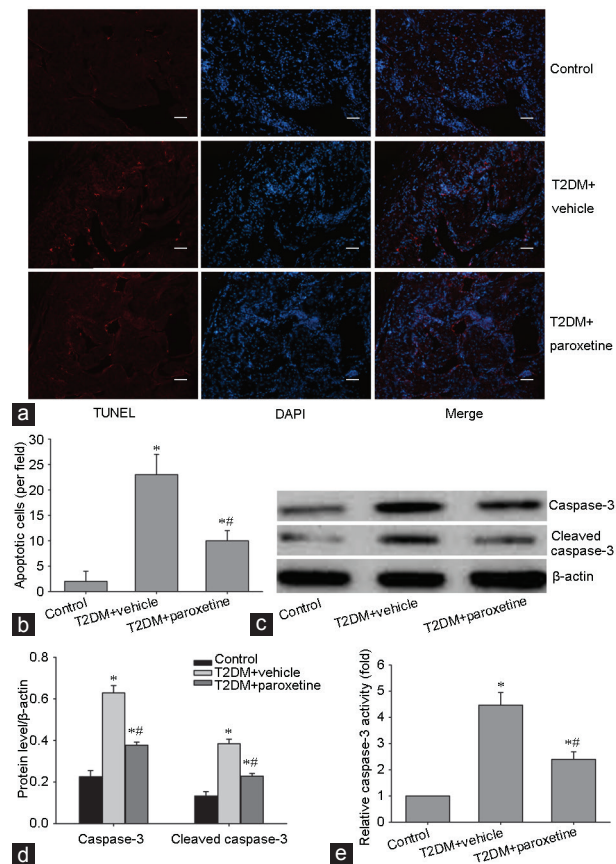


**Figure 6:** Effect of GRK2 inhibition on apoptosis. (a) The corpus cavernosum was stained with terminal deoxynucleotidyl transferase (TdT)-mediated dUTP nick end-labeling (TUNEL, red) and 4,6-diamidino-2-phenylindole (DAPI, blue) for apoptotic cells and cell nuclei, respectively (magnification ×200, scale bars = 50 μm). (b) Bar graphs represent quantitative image analysis for TUNEL assay. (c) Caspase-3 and cleaved caspase-3 protein expression was measured by western blot analysis. β-actin was used as a loading control. (d) Expression levels of caspase-3 and cleaved caspase-3 protein were normalized to β-actin. (e) Caspase-3 activity was presented as the fold change relative to the non-diabetic controls. Results were reported as mean ± standard deviation (s.d.). \**P* < 0.05, the indicated group versus control group; #*P* < 0.05, the indicated group versus T2DM+vehicle group; *n* = 20 per group. All results are representative of three independent experiments. GRK2: G protein-coupled receptor kinase 2; T2DM: type 2 diabetes mellitus.

There are several limitations in our study. First, it has been reported that paroxetine binds directly to GRK2 and inhibits kinase activity,<sup>23</sup> while the mechanism by which paroxetine decreases GRK2 expression remains unknown and requires further investigation. Second, the mechanism underlying how the upregulated GRK2 in CC affects Akt activation needs to be further elucidated. Recent data highlight a potential mechanism by which enhanced GRK2 can antagonize the action of β-arrestin 2, which acts as a scaffold for the interface of Akt and the insulin receptor and facilitates insulin signaling, thus attenuating Akt/eNOS phosphorylation and NO production.<sup>20</sup> Third, considering the selective serotonin reuptake inhibitor (SSRI) activity of paroxetine, it is probable that chronic paroxetine treatment in nondepressed T2DM patients would not be practical. However, observations of this study shed some light on the hypothesis that overexpressed GRK2 correlates with T2DM ED and novel drugs for GRK2-specific targeting might be promising therapies.

In conclusion, this study provides evidence for the role of GRK2 activation in the pathogenesis of T2DM ED, whereas a GRK2 inhibitor ameliorated the Akt/eNOS pathway, restored NO production, downregulated NADPH oxidase, subsequently inhibited ROS generation and apoptosis, and ultimately preserved erectile function. GRK2 inhibition may be a potential therapeutic strategy for T2DM ED by preserving endothelial function and preventing oxidative stress in cavernosal tissue.

#### AUTHOR CONTRIBUTIONS

ZHW and YJZ designed the study, analyzed and interpreted the experimental data and drafted and revised the manuscript. ZHW, YJZ, GH, DW and YW carried out the studies and collected the experimental data. ZHW, YJZ and YLG performed the statistical analysis. LC conceived of the study, and participated in its design and coordination. All authors read and approved the final manuscript.

#### COMPETING INTERESTS

The authors declare no competing interests.

#### REFERENCES

- Kouidrat Y, Pizzolo D, Cosco T, Thompson T, Carnaghi M, *et al*. High prevalence of erectile dysfunction in diabetes: a systematic review and meta-analysis of 145 studies. *Diabet Med* 2017; 34: 1185–92.
- Penson DF, Latini DM, Lubeck DP, Wallace KL, Henning JM, *et al*. Do impotent men with diabetes have more severe erectile dysfunction and worse quality of life than the general population of impotent patients? Results from the Exploratory Comprehensive Evaluation of Erectile Dysfunction (ExCEED) database. *Diabetes Care* 2003; 26: 1093–9.
- Redrow GP, Thompson CM, Wang R. Treatment strategies for diabetic patients suffering from erectile dysfunction: an update. *Expert Opin Pharmacother* 2014; 15: 1827–36.
- Hidalgo-Tamola J, Chitale K. Type 2 diabetes mellitus and erectile dysfunction. *J Sex Med* 2009; 6: 916–26.
- Luttrell IP, Swee M, Starcher B, Parks WC, Chitale K. Erectile dysfunction in the type II diabetic db/db mouse: impaired venoocclusion with altered cavernosal vasoreactivity and matrix. *Am J Physiol Heart Circ Physiol* 2008; 294: H2204–11.
- Carneiro FS, Giachini FR, Carneiro ZN, Lima VV, Ergul A, *et al*. Erectile dysfunction in young non-obese type II diabetic Goto-Kakizaki rats is associated with decreased eNOS phosphorylation at Ser1177. *J Sex Med* 2010; 7: 3620–34.
- Villalba N, Martinez P, Briones AM, Sanchez A, Salaices M, *et al*. Differential structural and functional changes in penile and coronary arteries from obese Zucker rats. *Am J Physiol Heart Circ Physiol* 2009; 297: H696–707.
- Long T, Liu G, Wang Y, Chen Y, Zhang Y, *et al*. TNF- $\alpha$ , erectile dysfunction, and NADPH oxidase-mediated ROS generation in corpus cavernosum in high-fat diet/streptozotocin-induced diabetic rats. *J Sex Med* 2012; 9: 1801–14.
- Zhang W, Fu F, Tie R, Liang X, Tian F, *et al*. Alpha-linolenic acid intake prevents endothelial dysfunction in high-fat diet-fed streptozotocin rats and underlying mechanisms. *Vasa* 2013; 42: 421–8.
- Silva FH, Lanaro C, Leiria LO, Rodrigues RL, Davel AP, *et al*. Oxidative stress associated with middle aging leads to sympathetic hyperactivity and downregulation of soluble guanylyl cyclase in corpus cavernosum. *Am J Physiol Heart Circ Physiol* 2014; 307: H1393–400.
- Jin L, Burnett AL. NADPH oxidase: recent evidence for its role in erectile dysfunction. *Asian J Androl* 2008; 10: 6–13.
- Burnett AL, Musicki B, Jin L, Bivalacqua TJ. Nitric oxide/redox-based signalling as a therapeutic target for penile disorders. *Expert Opin Ther Targets* 2006; 10: 445–57.
- Musicki B, Hannan JL, Lagoda G, Bivalacqua TJ, Burnett AL. Mechanistic link between erectile dysfunction and systemic endothelial dysfunction in type 2 diabetic rats. *Andrology* 2016; 4: 977–83.

- Guccione M, Ettari R, Taliani S, Da Settimo F, Zappala M, *et al*. G-protein-coupled receptor kinase 2 (GRK2) inhibitors: current trends and future perspectives. *J Med Chem* 2016; 59: 9277–94.
- Liu S, Premont RT, Kontos CD, Zhu S, Rockey DC. A crucial role for GRK2 in regulation of endothelial cell nitric oxide synthase function in portal hypertension. *Nat Med* 2005; 11: 952–8.
- Mayor F Jr, Lucas E, Jurado-Pueyo M, Garcia-Guerra L, Nieto-Vazquez I, *et al*. G Protein-coupled receptor kinase 2 (GRK2): a novel modulator of insulin resistance. *Arch Physiol Biochem* 2011; 117: 125–30.
- Vila-Bedmar R, Cruces-Sande M, Lucas E, Willems HL, Heijnen CJ, *et al*. Reversal of diet-induced obesity and insulin resistance by inducible genetic ablation of GRK2. *Sci Signal* 2015; 8: ra73.
- Garcia-Guerra L, Nieto-Vazquez I, Vila-Bedmar R, Jurado-Pueyo M, Zalba G, *et al*. G protein-coupled receptor kinase 2 plays a relevant role in insulin resistance and obesity. *Diabetes* 2010; 59: 2407–17.
- Taguchi K, Matsumoto T, Kamata K, Kobayashi T. G protein-coupled receptor kinase 2, with  $\beta$ -arrestin 2, impairs insulin-induced Akt/endothelial nitric oxide synthase signaling in ob/ob mouse aorta. *Diabetes* 2012; 61: 1978–85.
- Taguchi K, Matsumoto T, Kamata K, Kobayashi T. Inhibitor of G protein-coupled receptor kinase 2 normalizes vascular endothelial function in type 2 diabetic mice by improving  $\beta$ -arrestin 2 translocation and ameliorating Akt/eNOS signal dysfunction. *Endocrinology* 2012; 153: 2985–96.
- Fan Q, Chen M, Zuo L, Shang X, Huang MZ, *et al*. Myocardial ablation of G protein-coupled receptor kinase 2 (GRK2) decreases ischemia/reperfusion injury through an anti-intrinsic apoptotic pathway. *PLoS One* 2013; 8: e66234.
- Theccanat T, Philip JL, Razzaque AM, Ludmer N, Li J, *et al*. Regulation of cellular oxidative stress and apoptosis by G protein-coupled receptor kinase-2; the role of NADPH oxidase 4. *Cell Signal* 2016; 28: 190–203.
- Thal DM, Homan KT, Chen J, Wu EK, Hinkle PM, *et al*. Paroxetine is a direct inhibitor of g protein-coupled receptor kinase 2 and increases myocardial contractility. *ACS Chem Biol* 2012; 7: 1830–9.
- Chiou WF, Liu HK, Juan CW. Abnormal protein expression in the corpus cavernosum impairs erectile function in type 2 diabetes. *BJU Int* 2010; 105: 674–80.
- Albersen M, Lin G, Fandel TM, Zhang H, Qiu X, *et al*. Functional, metabolic, and morphologic characteristics of a novel rat model of type 2 diabetes-associated erectile dysfunction. *Urology* 2011; 78: 476.e1–8.
- Wan ZH, Li GH, Guo YL, Li WZ, Chen L. Calcipain inhibition improves erectile function in a rat model of cavernous nerve injury. *Urol Int* 2015; 95: 233–9.
- Wan ZH, Li WZ, Li YZ, Chen L, Li GH, *et al*. Poly(ADP-Ribose) polymerase inhibition improves erectile function in diabetic rats. *J Sex Med* 2011; 8: 1002–14.
- Livak KJ, Schmittgen TD. Analysis of relative gene expression data using real-time quantitative PCR and the 2<sup>-</sup>(Delta Delta C(T)) method. *Methods* 2001; 25: 402–8.
- Hupfeld CJ, Olefsky JM. Regulation of receptor tyrosine kinase signaling by GRKs and beta-arrestins. *Annu Rev Physiol* 2007; 69: 561–77.
- Penela P, Murga C, Ribas C, Lafarga V, Mayor F Jr. The complex G protein-coupled receptor kinase 2 (GRK2) interactome unveils new physiopathological targets. *Br J Pharmacol* 2010; 160: 821–32.
- Penela P, Rivas V, Salcedo A, Mayor F Jr. G protein-coupled receptor kinase 2 (GRK2) modulation and cell cycle progression. *Proc Natl Acad Sci U S A* 2010; 107: 1118–23.
- Kawakami T, Urakami S, Hirata H, Tanaka Y, Nakajima K, *et al*. Superoxide dismutase analog (Tempol: 4-hydroxy-2, 2, 6, 6-tetramethylpiperidine 1-oxyl) treatment restores erectile function in diabetes-induced impotence. *Int J Impot Res* 2009; 21: 348–55.
- Ceriello A. New insights on oxidative stress and diabetic complications may lead to a “causal” antioxidant therapy. *Diabetes Care* 2003; 26: 1589–96.

This is an open access journal, and articles are distributed under the terms of the Creative Commons Attribution-NonCommercial-ShareAlike 4.0 License, which allows others to remix, tweak, and build upon the work non-commercially, as long as appropriate credit is given and the new creations are licensed under the identical terms.

©The Author(s)(2018)

